J Solid State Eletrochem (2004) 8: 308–315
DOI 10.1007/s10008-003-0454-0

ORIGINAL PAPER

Henryk Scholl · Tadeusz Blaszczyk
Andrzej Leniart · Krzysztof Polanski

Nanotopography and electrochemical impedance spectroscopy of palladium deposited on different electrode materials

Received: 8 January 2003 / Accepted: 4 August 2003 / Published online: 21 November 2003

Abstract The objective of this work was to describe the characteristics of chemically and electrochemically deposited Pd surface layers on HOPG and polycrystalline gold electrode, using in situ ECSTM and EIS measurements, and SEM-EDX element analysis. Pd surface layers were deposited, in successive voltammetric cycles, and anodically dissolved in 0.01 M HCl + 0.01 M $(NH_4)_2PdCl_4$ aqueous electrolyte. Both of the electrode materials used in the study were treated as standard testing electrodes: (i) HOPG for STM/ECSTM measurements, and (ii) polycrystalline Au as the well known working electrode in various electro-analytical applications. The elements' surface analysis and nano-surface pictures were used to interpret the EIS diagrams and electrical equivalent circuits. Pd chemical and electrochemical deposition on the HOPG surface was compared with the same process on the polycrystalline gold electrode, on which palladium can be electrodeposited only by means of electrochemical cathodic deposition. Surface topographies of the electrodeposited palladium layers on HOPG and Au were completely different. The equivalent electrical circuits were fitted and the surface roughness of the investigated electrodes calculated. Relations between the surface topography, EIS and SEM-EDX, and interface model of the electrolyte solution | electrodeposited Pd layer | matrix electrode were proposed.

Keywords Pd deposition · HOPG and Au electrodes · EIS · SEM-EDX surface analysis

H. Scholl (✉) · T. Blaszczyk · A. Leniart
Department of General and Inorganic Chemistry,
University of Lodz, 68 Narutowicza str.,
90-136 Lodz, Poland
E-mail: hscholl@chemul.uni.lodz.pl
Tel.: +48 42 6355783
Fax: +48 42 6783958

K. Polanski
Department of Solid State Physics, University of Lodz,
149/153 Pomorska str., 90-236 Lodz, Poland

Introduction

Palladium is frequently used in the production of electronic devices as a first-step activation material, e.g., in the form of nanometric Pd particles deposited current-less on the substrate, which is the hol-array membrane on porous alumina in the polymer matrix [1]. The electrochemical properties of palladium electrodes are one of the most interesting contemporary subjects. Especially, their large hydrogen absorption capacity, application in fuel cells, and electrochemical reduction of different chemical substrates [2] draw considerable attention. Palladium cathodes received wide publicity due to the 'cold fusion' experiment [3]. The problem of tritium evolution reaction from D_2O or LiOD solutions on Pd cathode was later described by many authors, e.g. [4].

Supported noble metals catalysts on carbon or other noble metals are widely used in the chemical industry for hydrogeneration reactions. The efficiency of those catalysts, in particular their selectivity and activity, depends critically on the metallic clusters' size, distribution, oxidation state, and interaction with their support—in our case with highly oriented pyrolitic graphite (HOPG). A group of studies investigating Pd clusters on HOPG substrate, using STM, AFM or other surface investigation techniques, focused on materials obtained by means of high vacuum nucleates or a low-energy cluster beam [5, 6, 7, 8, 9, 10, 11]. Pd particle size, deposited electrochemically, is lower than obtained via atomic beam deposition. Particles concentrate in clusters with a size distribution centered around 50 atoms. They are mobile on the substrate, diffuse, and dynamically coalesce to form larger particles [5]. Isolated clusters are triangular and hexagonal in shape. Two-dimensional Pd islands were also observed near 3D clusters. They were composed of a six-fold symmetric lattice of Pd atoms with parameter of 0.42 nm. The majority of cited researches suggest a strong interaction between Pd atoms and HOPG surface. They show how the surface electronic

structure affects the size of single particles that strongly interact with the conductive HOPG surface [5, 6, 7, 8, 9, 10]. It is interesting, however, to note that Murakami et al. [11] suggest weak Pd–HOPG interaction.

The spontaneous deposition of palladium on conductive and non-catalytic, non-metallic HOPG surface has not yet been described, whereas, for platinum the same deposition mechanism on HOPG, from acetonitrile solution of $PtCl_6^{2-}$, has been extensively discussed [12].

Itaya [13] described oxidation dependencies of the Pd monocrystals in iodine-free 0.05 M H_2SO_4 solutions and noted that the anodic peak was related to the simple two-electron dissolution reaction:

$$Pd_{(s)} \rightarrow Pd^{2+}_{(aq)} + 2e \quad (1)$$

In STM, the characteristics of single crystals—flat terraces with monoatomic steps, intercepting one another at an angle of 60 ° or 120 ° were described. It was also noted that gradual island dissolution occurred. Dissolution occurs along the substrate or, in case of I^- ion adsorption, adsorbed atomic rows. The dissolution mechanism is a step-selective layer-by-layer type [13].

The electrodeposition of Pd, controlled by in situ STM observation, onto unreconstructed Au(100) monocrystals, was described by Kolb et al. [14]. In this paper the Pd growth mechanism on island-covered Au(100) is markedly different from that on island-free surface. They observed also that thicker Pd overlayers have very similar surface properties to those of massive Pd(100) single crystals. The same electrodeposition processes were observed by Uosaki et al. [15] on the Au(111) monocrystal electrode where Pd deposition proceeded by an instantaneous nucleation and two-dimensional growth mode.

In the literature, the Pd electrodeposition process on polycrystalline gold surface has still not been fully described. The polycrystalline gold electrode is one of the standard electrodes in electrochemical and electroanalytical measurements. The objective of this study was to describe the fundamental processes of palladium electrodeposition on a gold electrode and to explain the behavior of the palladium layer.

Experimental

Electrochemical scanning tunneling microscopy (ECSTM) measurements were carried out with a home-made apparatus based on the CAMAC system [16, 17, 18]. The Pt/Ir(90/10) tip ($\varnothing = 0.25$ mm), etched electrochemically in 3 M NaCN + 1 M NaOH solution and isolated with Apiezon, was applied [19, 20]. During the in situ ECSTM measurements the faradaic current of the tip was $I_F < 0.1$ nA. The voltammetric curve plots (CV), deposition with charge control (in potentiostatic conditions), and electrochemical impedance spectroscopy (EIS) measurements were done with potentiostat (Autolab-Ecochemie) having a FRA2 module, in the same small electrochemical cell ($V \cong 2$ cm^3) that was used in ECSTM in situ experiments with a working electrode of $A = 0.2$ cm^2. This procedure assures good repeatability of the results [21]. A Pt, ring-shaped wire was applied as a counter electrode and a special miniature calomel electrode in NaCl saturated solution (potential of this electrode is $E_{SSCE} = 0.236$ V vs. standard hydrogen electrode) as a reference electrode. In this work all potentials were given vs. the reference electrode. The main diagram of the measurement system is shown in Fig. 1. The aqueous solution of 0.01 M HCl as supporting electrolyte and the working electrolyte 0.01 M $(NH_4)_2PdCl_4$ in triply distilled water were used in all measurements.

As working electrodes, a highly oriented pyrolitic graphite (HOPG) (Adv. Ceramics, USA) and polycrystalline gold (99.99%) electrode (Polish National Mint) were used. The HOPG electrode is frequently used as a test electrode, in various STM and ECSTM experiments, for surface layer nanostructure characterization of the deposited metals, alloys, and polymers. Sticking and detachment of a scotch-tape were used to clean the HOPG electrode surface.

A polycrystalline gold electrode is used in most electrochemical research as the test electrode, e.g., in electrolysis, investigations of metals and metal alloy mechanisms, and array of organic compound electrosynthesis in various aqueous and non-aqueous solvents. The Au electrode was polished mechanically (SiC abrasive paper; 2000 grain) and tested electrochemically in 0.5 M H_2SO_4 for obtaining the CV curve according to the literature data [22]. Before Pd electrodeposition, the Au electrode was activated in 0.01 M HCl solution, in 25 cycles. Ammonium tetrachloropalladium (II) (Ventron), hydrochloric acid HCl p.a. (POCH–Gliwice), and distilled/Millipore RQ water were employed. The deposition processes consisted of single cyclic voltammetric curve from the equilibrium potential to the first cathodic potential, and then depositions with charge control (under potentiostatic condition) and different charges. The dissolution process measurements were done differently: with cyclic voltammetric curves in anodic region of the potential polarization for HOPG, and with anodic charge control (under potentiostatic condition) for polycrystalline Au. The EIS spectra were measured in the equilibrium potential, in which the rejected steady-state current was equal to zero. Harmonic measuring signal was within the range 0.05 Hz to 10 kHz with $E_{AC} = 10$ mV.

Results and discussion

Palladium chemical and electrochemical deposition and dissolution on the HOPG electrode

Spontaneous, currentless Pd deposition on HOPG after immersion for 15 min in 0.01 M $(NH_4)_2PdCl_4$ solution was observed (Fig. 2a). Pd currentless deposition on HOPG may have similar character to spontaneous Pt deposition on the very same substrate. This process was described in detail by Peikang Shen et al. [12]. They found spontaneous creation of randomized Pt structures

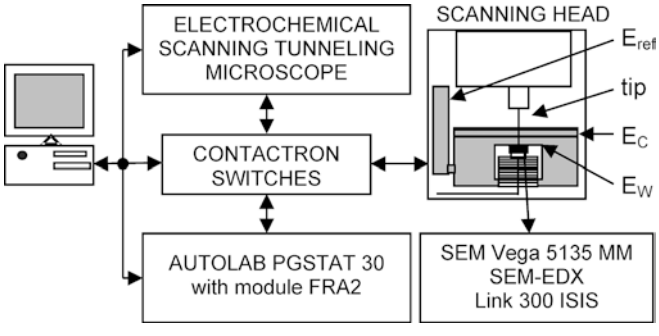

Fig. 1 Main diagram of the measurement methods and apparatus

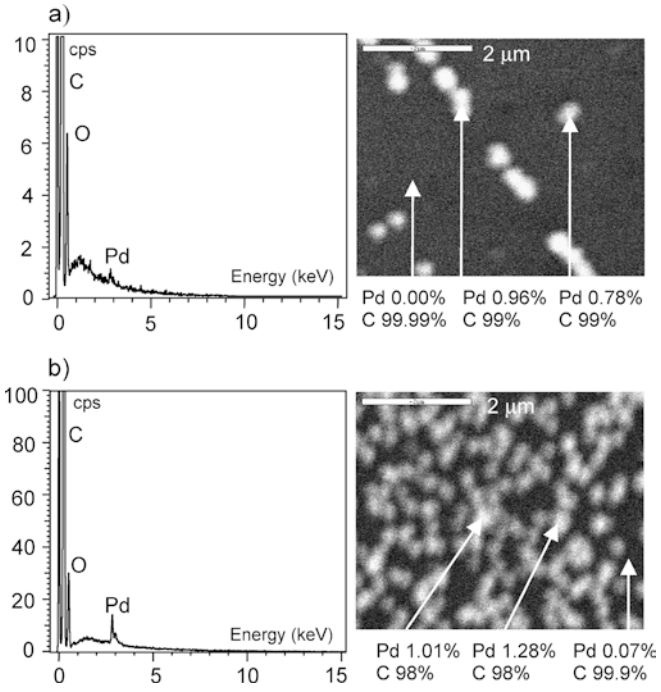

Fig. 2a,b Pd deposition on HOPG: SEM-EDX spectra and local elemental analysis **a** after currentless deposition (15 min in solution), and **b** after the first electrochemical cathodic deposition curve

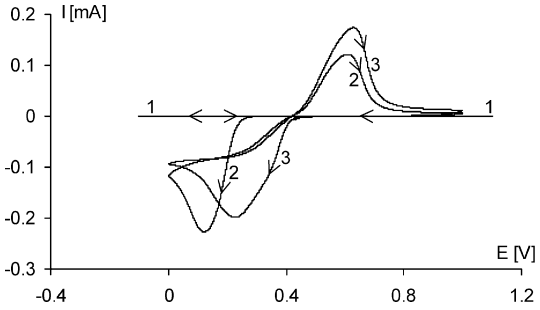

Fig. 3 Voltammetric characteristics of HOPG electrode: *1* in supporting 0.01 M HCl electrolyte, *2* after the 1st curve, *3* after the 3rd curve in 0.01 M HCl + 0.01 M $(NH_4)_2PdCl_4$ solution; potentials vs. saturated calomel electrode, $v = 10$ mV s^{-1}

after immersing the HOPG into CH_3CN solutions containing H_2PtCl_6. The reasons for such a process are still unclear. One could be the presence of oxidation centers on the fresh HOPG surface, with increased electron density on the terraces and crystallography jog border [12].

The weak interaction, described here, between HOPG surface and Pd particles was observed in other research on the dislocation jogs, whereas no palladium nuclei were observed on the flat region of activated surfaces [13, 23]. Figure 2a confirms that the preferential Pd deposition on HOPG occurs mainly on crystallographic jogs, created when cleaning the surface. As a reference, Fig. 2b illustrates the HOPG surface after the first cycle of palladium electrodeposition—palladium nuclei are randomly deposited on the active centers and the HOPG surface is partially modified.

CV curves of both electrodes immersed in the supporting electrolyte constitute a convenient environment for the observation of faradic processes analogous to reaction (1). In Fig. 3 the first Pd electrodeposited layer on HOPG is characterized by electrodeposition peak potential $E_{1p(dep)} = 0.13$ V and electrodissolution peak potential $E_{1p(dis)} = 0.61$ V ($\Delta E_{1p} = 0.48$ V). Charge relation below the anodic–cathodic curves of the first cycle equals $Q_{1(dis)}/Q_{1(dep)} = 0.34$. This relation suggests that a large part of the electrodeposited palladium atoms remains on the HOPG surface and that in the consecutive voltammetric processes electrodeposition occurs on the partially, non-continuously modified HOPG electrode. The 3rd subsequent cycle of the electrodeposition–electrodissolution processes is also presented in Fig. 3. It is characterized by the peak potentials of $E_{3p(dep)} = 0.24$ V and $E_{3p(dis)} = 0.61$ V ($\Delta E_{3p} = 0.37$ V). The cathodic voltammetric branch of the 3rd cycle in Fig. 3 at the potential $E \cong 0.34$ V may suggest a two-step electron process. The charge calculated below the curves increases along the consecutive cycles, up to the relation $Q_{3(dis)}/Q_{3(dep)} = 0.41$.

The HOPG surface in the chemical Pd deposition is slightly modified by Pd atoms during the first electrochemical deposition cycle and this fact has consequences in the subsequent ones. Figure 4 presents ECSTM pictures (2611 nm×2611 nm) obtained after palladium electrodeposition under the coulostatic control at $E_{(dep)}$ potential. Palladium deposited electrochemically creates structures, having the characteristic form of crystallites, independent of the HOPG surface electrode (Fig. 4b). Additionally, Pd electrodeposited on the HOPG has weak adhesive properties to the HOPG electrode.

The surface roughness amounts to a constant value after Pd electrodeposition under $Q = -0.373$ C (Fig. 4c). The surface roughness σ, proposed by W. U. Schmidt et al. [24], is a standard deviation of the values of differences between the height of the real surface and the arbitrary plane (the best plane for real surface) and is calculated as shown:

$$\sigma = \sqrt{\left\langle [H(x,y) - \langle H(x,y)\rangle]^2 \right\rangle} \qquad (2)$$

where $H(x,y)$ is the height of the real surface and $< H(x,y) >$ is the height of the point on arbitrary plane and lies at the same x,y ordinates.

Figures 5a,b show impedance plots, measured in equilibrium potential, recalculated per geometric area unit of the HOPG electrode surface, after the first CV and consecutive cycles of electrodeposition processes under the coulometric control, and after anodic dissolution. Based on the gathered results, the following model (Fig. 6) could be proposed, describing the investigated interface system for both the HOPG and Au respectively:

Electrolyte solution | Palladium deposited layer | Matrix working electrode (HOPG or polycrystalline Au)

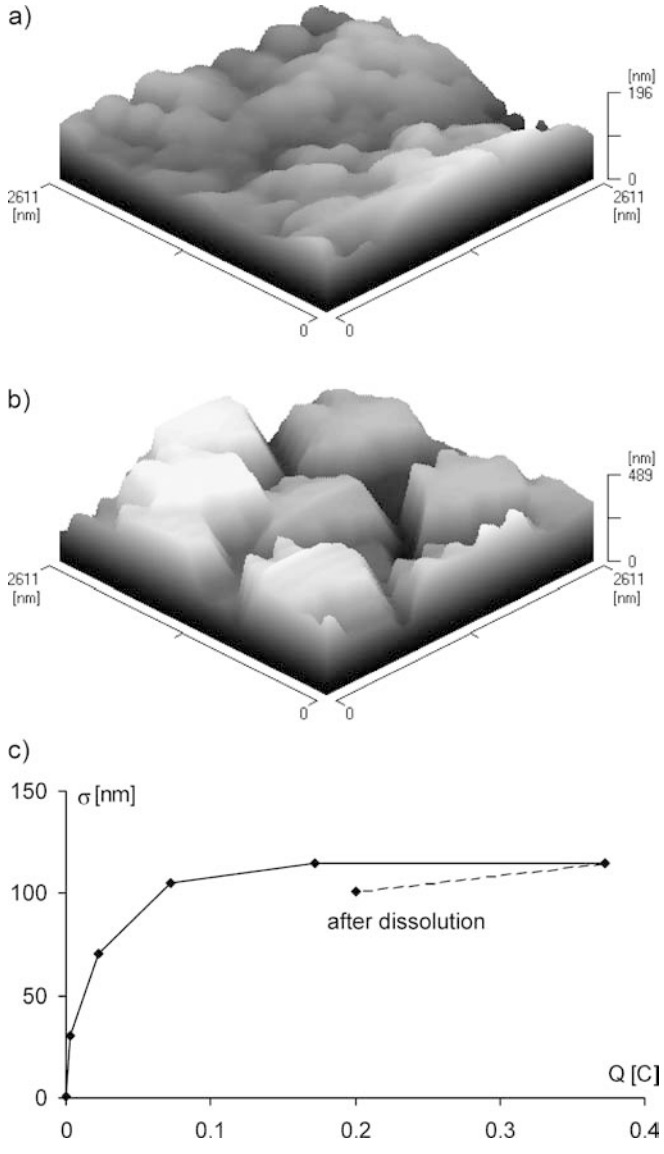

Fig. 4a–c Pd electrodeposition on HOPG **a** after the first electrochemical cathodic deposition curve ($Q_1 = -0.003$ C) and **b** after $Q_5 = -0.373$ C. **c** Surface roughness σ vs. charge Q_i

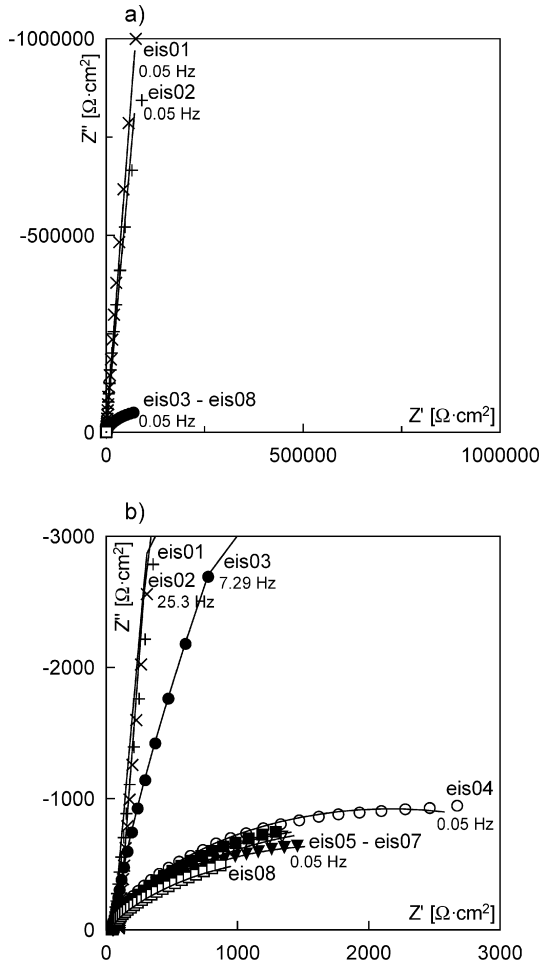

Fig. 5a,b EIS spectra ($E = 0.45$ V, $I_{DC} < 0.3$ μA) of Pd deposited surface layer on HOPG and Pd dissolved from HOPG: **a**, **b** Nyquist plots (× eis01, + eis02, ● eis03, ○ eis04, ▼ eis05, ▽ eis06, ■ eis07, □ eis08, after the 2nd curves of anodic dissolution)

Elements in this model can be interpreted as follows: R_S-typical uncompensated solution resistance between working and reference electrodes, R-resistance of oxidation–reduction reactions connecting with changes of Pd coverage, C-double layer capacitance and CPE1-constant phase element that represents the electrical properties of the Pd layer.

The results indicate that impedances in the supporting 0.01 M HCl and containing 0.01 M $(NH_4)_2PdCl_4$ solutions, before electrodeposition, are similar (eis01 and eis02 in Fig. 5 and Table 1). They can be modulated with a simplified circuit containing no C and R elements. This means that the spontaneous Pd deposition influences the impedance to a lesser degree. After the first cathodic curve ($Q_1 = -0.003$ C) the impedance steeply decreases (eis03). For the consecutive Pd electrodepositions, beginning with $Q_2 = -0.023$ C (eis04 to eis07), impedances differed only slightly. Presented changes may be related to the HOPG layering:

– After the first cathodic curve, the Pd layer is not continuous
– After $Q_2 = -0.023$ C the Pd layer is continuous, whereas, the following layers grow uniformly on underlying ones.

The changes of the electrical equivalent circuit parameters may be attributed to changes in the layering process and especially to an increase in roughness (C and CPE1-T values increase with an almost constant CPE1-P value clearly less than 1). Polarization resistance R decreases markedly after continuous Pd layer formation. After Pd dissolution $Q_{(dis)} = 0.010$ C, the form of the impedance curve (eis08) is similar to the form of eis04–eis07 curves. This fact could be explained by assuming that the Pd layer dissolves uniformly. Attempts at Pd dissolution showed that the deposited Pd cannot be removed entirely from the HOPG surface. Pd atoms are built into the HOPG structure and permanently change its surface properties.

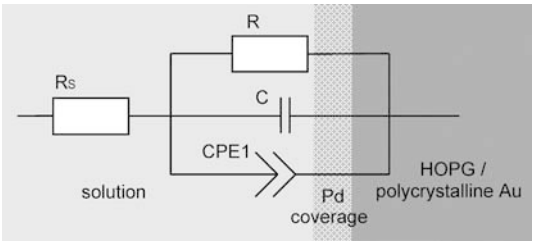

Fig. 6 Model of the HOPG and Au electrodes modified by palladium electrodeposited and stabilized layer after 3–5 cycles of electrodeposition–electrodissolution

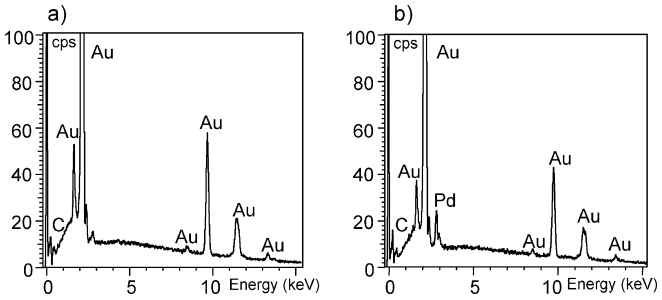

Fig. 7a,b Pd deposition on polycrystalline Au: SEM-EDX spectra and local elemental analysis **a** after currentless deposition (15 min in solution), and **b** after the first electrochemical cathodic deposition curve

It is worth underlining that the impedance changes behave similarly to surface roughness σ changes (shown in Fig. 4).

Palladium chemical and electrochemical deposition and dissolution on the polycrystalline gold electrode

On the polycrystalline gold electrode, chemical deposition of palladium could not be observed (Fig. 7a). Pd deposition on gold may only occur in the process of cathodic electrodeposition (Fig. 7b).

This process is illustrated by the cyclic voltammograms shown in Fig. 8, where different plots of the CV curves of palladium electrodeposition are described by potential peak values $E_{1p(dep)} = 0.22$ V and $E_{1p(dis)} = 0.58$ V ($\Delta E_{1p} = 0.36$ V) for the first cycle, whereas for the last cycle $E_{5p(dep)} = 0.24$ V and $E_{5p(dis)} = 0.51$ V ($\Delta E_{5p} = 0.27$ V). For all cycles, the charges relation was stable and equaled $Q_{(dis)}/Q_{(dep)} = 0.52$. This relation suggests two behavior possibilities of the deposited surface layers: the palladium atoms remain in matrix dislocations of the gold electrode surface, or modification occurs on the surface by formation of Au_xPd_y alloys. The EDX analysis cannot define the x/y relation as the answer signal contains the echo of the gold groundmass.

The 5th cycle curve course of the cathodic palladium deposition in $E = 0.36$ V shows the affinity with the same curve branch presented in Fig. 3 for HOPG electrode (in $E = 0.34$ V). This fact, and the chemical behavior of the $[PdCl_4^{2-}]$ complex, suggest a more complicated mechanism of the electrodeposition reaction on the surfaces with electrodeposited Pd layer. In this mechanism the tetrachloride palladium complex

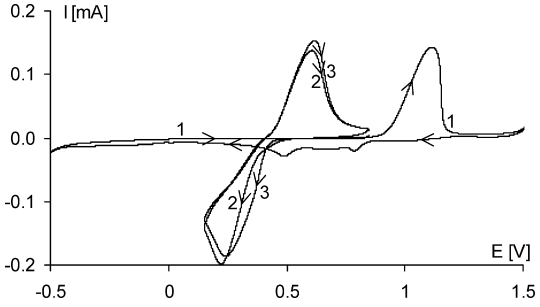

Fig. 8 Voltammetric characteristics of polycrystalline Au electrode: *1* in supporting 0.01 M HCl electrolyte, *2* after the 1st curve, and *3* after the 5th curve in 0.01 M HCl + 0.01 M $(NH_4)_2PdCl_4$ solution; potentials vs. saturated calomel electrode, $v = 10$ mV s^{-1}

stability, in the successive steps of its dissociation, and the influence of Cl^- anions of the 0.01 M HCl supporting electrolyte, must be taken into consideration. The four-step dissociation of $[PdCl_4^{2-}]$ in water was investigated many years ago [25, 26, 27] as the process where the palladium compounds $[Pd^{2+}] \Longleftrightarrow [PdCl^+] \Longleftrightarrow [PdCl_2] \Longleftrightarrow [PdCl_3^-] \Longleftrightarrow [PdCl_4^{2-}]$ were present in the equilibrium state described by four dissociation constants. The values [27] of $\log\beta_i$ in 1 M $HClO_4$ (spectroscopic method) equal $\log\beta_1 = 4.47$, $\log\beta_2 = 7.76$, $\log\beta_3 = 10.2$ and $\log\beta_4 = 11.5$, respectively. In this experiment, the electrolyte solution of $(NH_4)_2PdCl_4$ ($c = 0.01$ M in 0.01 M HCl supporting electrolyte) was used. The $[Pd^{2+}]$ ion concentration may be assumed to be equal to 0.01 M. In the cathodic deposition of

Table 1 Parameters of electrical equivalent circuit after Pd deposition and dissolution on HOPG

	Curve	Q_i (C)	R_s (Ω cm^2)	C (F cm$^{-2}\times10^{-6}$)	R (Ω cm^2)	CPE1-T ($\times10^{-6}$)	CPE1-P
0.01 M HCl	eis01	0	96.7	–	–	3.10	0.952
Deposition	eis02	0	55.6	–	–	3.67	0.944
	eis03	−0.003	56.4	4.36	141040	13.3	0.663
	eis04	−0.023	54.9	26.6	4540	302	0.463
	eis05	−0.073	57.2	53.1	3458	617	0.436
	eis06	−0.173	50.0	74.6	4169	716	0.441
	eis07	−0.373	49.8	80.4	3585	721	0.497
Dissolution	eis08	0.010	43.7	83.7	2805	1130	0.452

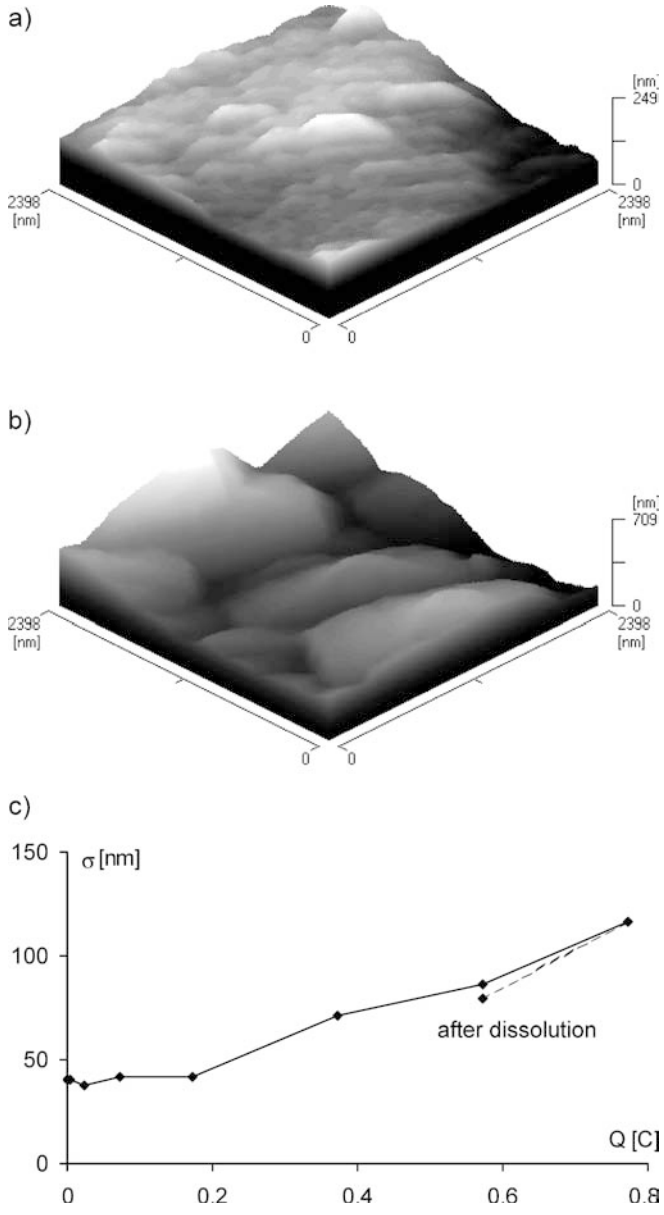

Fig. 9a–c Pd electrodeposition and electrodissolution on polycrystalline Au **a** after the first electrochemical cathodic deposition curve ($Q_1 = -0.003$ C) and **b** after $Q_7 = -0.773$ C. **c** Surface roughness σ vs. charge Q_i

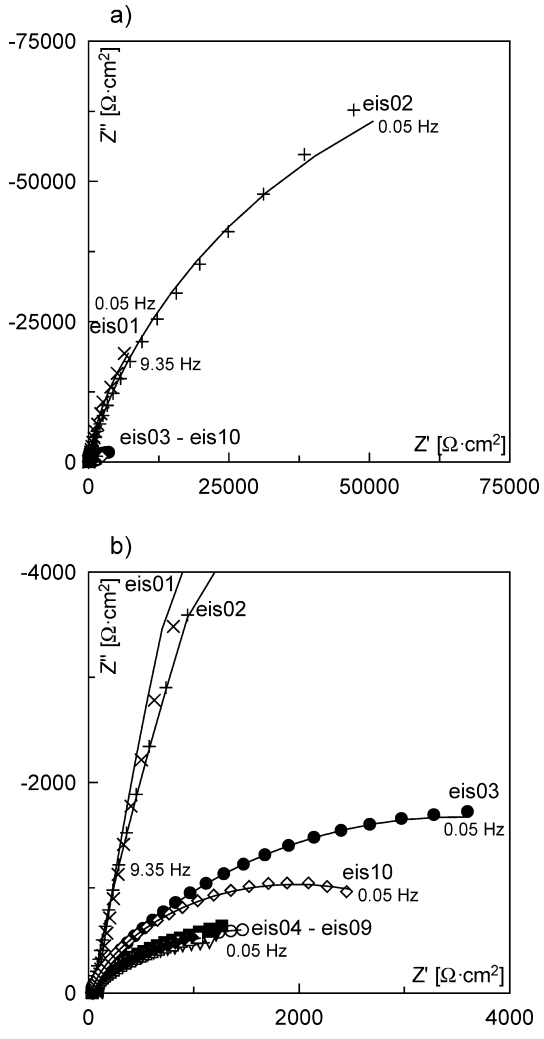

Fig. 10a,b EIS spectra ($E = 0.44$ V, $I_{DC} < 0.6$ μA) of Pd surface layers deposited and dissolved on polycrystalline Au: **a**, **b** Nyquist plots (× eis01, + eis02, ● eis03, ○ eis04, ▼ eis05, ▽ eis06, ■ eis07, □ eis08, ♦ eis09, ◇ eis10, after anodic dissolution)

palladium on HOPG and Au electrodes, the electrodeposition mechanism, judging by the curve fold of the cathodic branch, can be described as follows:

$$Pd^{2+} + e \Rightarrow Pd^{+} \quad \text{in } E = 0.36 \text{ V} \tag{3}$$

$$Pd^{+} + e \Rightarrow Pd^{0} \quad \text{in } E_{(dep)} = 0.24 \text{ V} \tag{4}$$

The ECSTM picture of the polycrystalline gold electrode matrix (Fig. 9a) shows regularly corrugated surface with the height approaching 250 nm. The first CV cycle and the subsequent ones, under coulometric control, show that cathodic deposition processes cause surface layer growth up to the height of about 500 nm. At the deposition beginning, the Pd coverage reproduces the Au matrix surface topography. A higher cathodic charge of cathodic deposition (Fig. 9b) causes the growth of the rougher surface.

The surface layer roughness (Fig. 9c) presented in the form of the function $\sigma = f(Q)$, suggests a linear dependence of the topography changes with the charge, contrary to HOPG, where the σ value was stable. The electrodeposited surface of Pd coverage does not dissolve completely under the charge $Q_{(dis)} = 0.200$ C. It causes insignificant smoothing of the surface, illustrated by the last point of $\sigma = f(Q)$ function. It is worth mentioning that no complete dissolution of Pd coverage on Au electrode was possible. This shows that Pd atoms modified the Au surface. Furthermore, formation of the intermetallic alloy-type Au_xPd_y complexes was possible. Nichols et al. [28] noticed a similar process of alloying with Cu deposition on monocrystallic Au.

Table 2 Parameters of electrical equivalent circuit after Pd deposition and dissolution on polycrystalline Au

	Curve	Q_i (C)	R_s (Ω cm^2)	C (F cm$^{-2}\times10^{-6}$)	R (Ω cm^2)	CPE1-T ($\times10^{-6}$)	CPE1-P
0.01 M HCl	eis01	0	78.33	–	100530	132	0.909
Deposition	eis02	0	44.84	7.38	206990	19.0	0.735
	eis03	−0.003	44.42	23.0	7208	251	0.531
	eis04	−0.023	44.30	38.3	3122	636	0.454
	eis05	−0.073	46.31	50.7	3170	823	0.436
	eis06	−0.173	47.71	56.7	2567	822	0.444
	eis07	−0.373	37.23	67.4	3673	789	0.436
	eis08	−0.573	34.29	82.4	3294	976	0.422
	eis09	−0.773	32.10	94.3	3637	1050	0.417
Dissolution	eis10	0.200	32.07	54.5	4194	313	0.531

The EIS plots (Fig. 10a,b) describe the electrochemical characteristics of the investigated solution | deposited Pd | Au electrode surface, before and after the palladium electrodeposition–electrodissolution processes. The fitted electrical equivalent circuit is presented in Fig. 6, and element values in Table 2.

Impedance behavior during electrochemical Pd deposition on Au is similar to the Pd deposition on HOPG described above. It is, though, difficult to explain major differences between impedances in the supporting electrolyte (eis01), and investigated solution containing 0.01 M $(NH_4)_2PdCl_4$ (eis02). SEM-EDX analysis showed no spontaneous Pd deposition on polycrystalline Au. Neither were there evident differences in the topography of the same area in the supporting electrolyte and investigated solution. Those major differences, for electrical equivalent circuit, are shown in Table 2. As mentioned above, after the first cathodic Pd electrodeposition curve and after consecutive charges Q_i, the characteristics of the impedance changes (from eis03 to eis09) and values of the electrical equivalent circuit elements are similar to HOPG. It is evident that the C values increase after each Pd electrodeposition cycle. CPE1-P and CPE1-T values raise analogically but not monotonically. Similar to HOPG, CPE1-P values are markedly lower than 1, whereas the resistance R (from eis04 up) oscillates around values close to the HOPG. After Pd coverage dissolution (with charge $Q = 0.200$ C), accompanied by almost double decrease in C values and triple in CPE1-T, the impedance increases (eis10). The changes might be explained by the dissolution of the most prominent coverage peaks.

It is worth underlining that, contrary to HOPG, for polycrystalline Au the results of the impedance measurements do not correlate with the results of the topography measurements for both Pd layer deposition and dissolution.

Conclusions

The method used in this study has provided extensive characterization of the palladium electrolyte | HOPG (or polycrystalline Au) electrode systems, using in situ ECSTM, voltammetric, and EIS investigations. Based on the results the following may be concluded:

1. Chemical deposition of palladium on the investigated HOPG solid electrode takes place at the surface dislocations or grains of terraces. Deposition on the polycrystalline gold palladium may only be obtained by electrochemical cathodic deposition processes.
2. The first chemically or electrochemically deposited Pd layer on HOPG is slightly attached to the matrix surface. The Pd multilayers electrodeposited on HOPG attach well and take the individual form, characteristic of palladium crystals. They multiply uniformly and the surface roughness σ achieves a constant value.
3. The first Pd layer electrodeposited on polycrystalline Au maps the matrix topography. The subsequent layers cause the surface development in the form of large and irregular structures. The roughness σ increases with every new Pd layer.
4. The course of the cathodic branches of the voltammetric curves after the 3rd–5th cycle suggest that at potential $E = 0.35$ V the Pd electrodeposition process on both modified electrodes can be seen as a two-step, one-electron process. In the anodic potential peaks, the palladium layer is partially dissolved and the charges of the electrodissolution–electrodeposition processes are < 1. This relation suggests penetration of Pd atoms into the surface dislocations and/or creation of Au_x/Pd_y alloys within the gold matrix.
5. The EIS plots, measured in the equilibrium potential, show that the palladium electrodeposition greatly influences the impedance characteristics of the matrix HOPG and Au electrodes, where the first cycle is considerably different in relation to the subsequent characteristics. Simulations of the electric equivalent circuits show that the presence of the CPE element is necessary in the electrical models. The EIS spectra and ECSTM pictures correlate strongly for HOPG, whereas for Au this correlation is not present.

Acknowledgement This study was supported by 505/247 Lodz University Grant.

References

1. Masuda H, Fukuda K (1999) J Electroanal Chem 473:240
2. Sakellaropoulos GP, Langer SH (1999) J Electrochem Soc 124:1548
3. Fleischman M, Pons S, Hawkins M (1989) J Electroanal Chem 261:301, (1989) ibid. 262:187
4. Brillas E, Esteve J, Sardin G, Casado J, Domenech X, Sanchez-Cabeza JA (1992) Electrochim Acta 37:215
5. Cadete Santos Aires FJ, Sautet P, Rousset JL (1994) J Vac Sci Technol B12:1776
6. Sartre A, Pahner M, Porte L, Sauvion GN (1993) Appl Surf Sci 70/71:402
7. Kojima I, Kurahashi M (1994) J Vac Sci Technol B12:1780
8. Humbert A, Dayez M, Sangay S, Chapon C, Henry CR (1990) J Vac Sci Technol A8:311
9. Bifone A, Casalis L, Riva R (1995) Physical Review 51:11043
10. Nie HY, Shimizu T (1994) J Vac Sci Technol B12:1843
11. Murakami Y, Naoi K, Yahikozawa K, Takasu Y (1994) J Electrochem Soc 141:2511
12. Peikang Shen, Ning Chi, Kwong-Yu Chan, Philips D (2001) Appl Surf Sci 172:159
13. Itaya K (1999) Atomic-scale aspects of anodic dissolution of metals: studies by in situ scanning tunneling microscopy. In: Wieckowski A. (ed) Interfacial electrochemistry. theory, experiment and applications. Dekker, New York, chap 12, pp 187–210 (and ref. therein)
14. Kibler L, Kleinert M, Kolb D (2000) Surf Sci 461:115
15. Quayum M, Shen Y, Uosaki K (2002) J Electroanal Chem 520:126
16. Blaszczyk T, Olejniczak W, Kobierski P (1995) Pomiary Automatyka Kontrola 12:342
17. Blaszczyk T, Kazmierczak D, Krzyczmonik P, Scholl H (1998) Polish J Chem 72:2134
18. Blaszczyk T, Kazmierczak D, Krzyczmonik P, Scholl H, Polanski K (2000) J Solid State Electrochem 4:95
19. Zhang B, Wang E (1994) Electrochim Acta 39:103
20. Melmed AJ (1991) J Vac Sci Technol B9:601
21. Scholl H, Blaszczyk T (2001) Proceedings 5th international symposium on electrochemical impedance spectroscopy, Marilleva. Italy, p 21
22. Piela B, Wrona PK (1995) J Electroanal Chem 388:69
23. Hwang BJ, Lin SH (1995) J Electrochem Soc 142:3749
24. Schmidt WU, Alkire RC, Gewirth AA (1966) J Electrochem Soc 143:3122
25. Gelfman MJ, Kiseleva NV (1964) Zhur Neorg Khim 14:179
26. Jackson E, Pantony DA (1971) J Appl Electrochem 1:283
27. Elding LJ (1972) Inorg Chim Acta 6:647
28. Nichols R, Beckmann W, Meyer H, Batina N, Kolb D (1992) J Electroanal Chem 330:381